Effect of Strain on the Properties of a Styrene–Butadiene Rubber Filled with Multiwall Carbon Nanotubes

Liliane Bokobza,[1] Colette Belin[2]

[1]Laboratoire PPMD, E.S.P.C.I., 10 rue Vauquelin, 75231 Paris, Cedex, France
[2]Laboratoire LPCM, Université de Bordeaux 1, 351, cours de la Libération, 33405 Talence, Cedex, France

ABSTRACT: Multiwall carbon nanotubes were dispersed in a styrene–butadiene copolymer. The effect of nanotube concentration on the tensile characteristics of the composites was examined. Electrical properties carried out under uniaxial extension show an increase in resistivity upon gradual stretching. A second stretch performed after total release of the stress was shown to lead to a flat response in resistivity. Atomic force microscopy was used to examine orientational effects and changes in filler structure occurring upon application of an uniaxial deformation. © 2007 Wiley Periodicals, Inc. J Appl Polym Sci 105: 2054–2061, 2007

Key words: carbon nanotubes; elastomers; mechanical properties; electrical properties

INTRODUCTION

Polymer nanocomposites have recently attracted intense scientific and technological interest because they often exhibit significantly enhanced properties when compared with the unfilled polymer or conventional composites at the same filler loading.[1–3]

Different nanoparticles morphologies have been used, including spherical particles, such as *in situ* generated silicas or highly anisotropic fillers like clay platelets or carbon nanotubes.[4–6]

The extent of reinforcement depends on the state of filler dispersion, the aspect ratio, and the degree of interaction with the polymer chains.[7,8]

The outstanding properties of carbon nanotubes (high tensile modulus, high electric conductivity, and high aspect ratio) make them ideal candidates for use in nanocomposites.[9] In addition to improved mechanical properties, carbon nanotubes also impart conductivity to the matrix.[10–14] The electrical conductivity depends on the filler concentration and the filler morphology such as particle size, structure as well as filler–filler and filler–matrix interactions, which determine the state of dispersion. The resistivity of conductive composites is also affected by a mechanical stretching that would cause an orientation of the bundles in the direction of stretch and also a breakage of the conductive pathways.[15,16]

This work reports investigations carried out on a styrene–butadiene rubber (SBR) filled with multiwall carbon nanotubes (MWNTs) or with carbon black (CB) for the sake of comparison. The effect of filler content on the stress–strain properties of the filled samples are discussed. On the other hand, the effect of strain on the electrical and mechanical properties of a filled material whose MWNTs content is above the percolation threshold, is considered.

EXPERIMENTAL

Materials

The styrene–butadiene rubber (SBR) contains 25 wt % of styrene units. The microstructure of the butadiene phase is the following: 10% cis, 17% trans, 73% 1,2. The formulations used in this work are shown in Table I. All the ingredients are in parts per hundred parts of rubber (phr).

MWNT, with an average outer diameter of about 10 nm and a length of $\sim$ 0.7 μm, were supplied by Nanocyl (Belgium). Carbon black (N330) was obtained from Cabot.

Appropriate quantities of carbon nanotubes were mixed in toluene by means of an Ultra-Turrax operating at 13,000–16,000 rpm until an observation with an optical microscope had revealed a homogeneous dispersion. The polymer and all the ingredients of formulation, were then dissolved in the suspension of carbon nanotubes and toluene under magnetic stirring at 300 rpm for about 12 h. After mixing, the toluene was carefully removed at 30°C under vacuum. The mix was cured in a standard hot press at 170°C for 10 min under a pressure of 150 Bars, in an electrically heated press. In this way, sheets of about

TABLE I
Formulations of the Rubber Compounds

Ingredients (phr)	SBR/MWNTs	SBR/CB
Rubber	100	100
Sulfur	1.1	1.1
Diphenyl guanidine (DPG)	1.45	1.45
Zinc oxide	1.82	1.82
Stearic acid	1.1	1.1
Cyclohexyl benzothiazole sulfenamide (CBS)	1.3	1.3
Multiwall carbon nanotubes (MWNTs)	0, 1, 2, 3, 5, 7, 10	
Carbon black (CB)		10, 50

200 μm (or around 1 mm for electrical measurements under strain) thickness were prepared.

Techniques

TEM images were obtained on a JEOL 100CXII. Pure carbon nanotubes were sonicated in toluene and droplets of the suspension were put onto copper grids for observation. Ultrathin films (60-nm thick) of the composite samples were cut by means of an ultramicrotome LEICA ULTRACUT UCT at −80°C by liquid nitrogen and put onto copper grids.

Atomic force microscopy (AFM) investigations were performed with a Thermomicroscope CP Research system, using tapping mode and phase imaging. The sample (around 200-μm thick) was put on a small stretching device specially fitted to the sample holder of the Multimode AFM. Topography, Error signal and phase images were simultaneously recorded to get a topographic and compositional mapping of the surface.

Electrical resistivity measurements were determined on samples of $10 \times 20 \times 0.2$ mm^3 by measuring their resistance on a high resistance meter (Keithley 6517A) between two conductive rubber electrodes with an alternative voltage of 1 V. This alternative voltage is needed to avoid a background current effect. The measured resistances R were then converted into volume resistivity ρ by using this equation:

$$\rho = \frac{RS}{d} \qquad (1)$$

where S is the cross-sectional area perpendicular to the current and d the thickness of the sample between the two electrodes.

The strain dependence of electrical resistivity was carried out on strips (size: $50 \times 15 \times 1$ mm^3) stretched with a manual stretching machine. Two clamps connected to the high resistance meter, were placed along the length of the specimen (Fig. 1). Measurements were made at about 5 min after each

elongation step. Electrical measurements during the second stretching were performed 1 h after the total unloading of the sample.

Under the assumption that the volume remains constant during deformation, the resistivity was obtained from the measured resistance, R, from the following expression:

$$\rho = \frac{R\,S_0}{\alpha^2 L_0} \qquad (2)$$

where S_0 and L_0 are the initial cross-sectional area and length between the two clamps, respectively and α is the extension ratio, which is the ratio of the length of the sample in the direction of strain to the initial length before deformation.

Strain–stress measurements were carried out at room temperature on strips of $50 \times 5 \times 0.2$ mm^3 between two clamps by means of a sequence of increasing weights attached to the lower clamp. The distance between two marks on the sample was measured with a cathetometer after allowing sufficient time (10 min after adding a weight) for equilibration. The second stretch for the evaluation of the stress-softening effect (Mullins effect) was performed 1 h after the total release of the stress.

RESULTS AND DISCUSSION

Morphology and dispersion of the MWNTs

TEM micrographs of MWNTs given in Figure 2, show a broad distribution in lengths and diameters which are in the ranges of 0.1–5–6 μm and 10–50 nm, respectively. They are highly entangled and exhibit a strong tendency to agglomerate into bundles, which reduce the effective aspect ratio.

The TEM images of the cryomicrotomed composite containing 4 phr of MWNTs (Fig. 3) reveal the presence of aggregates, which seem uniformly distributed in the matrix. A magnification of one bundle (Fig. 3 left) shows an orientation of the nano-
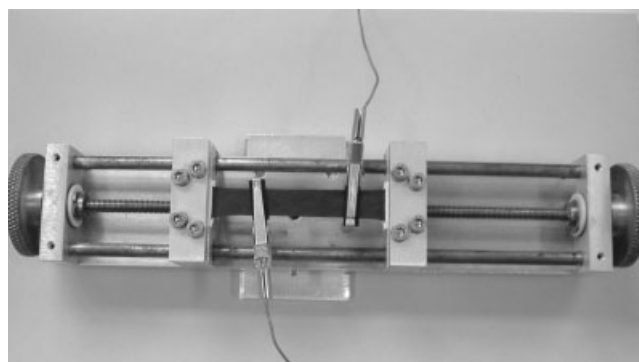

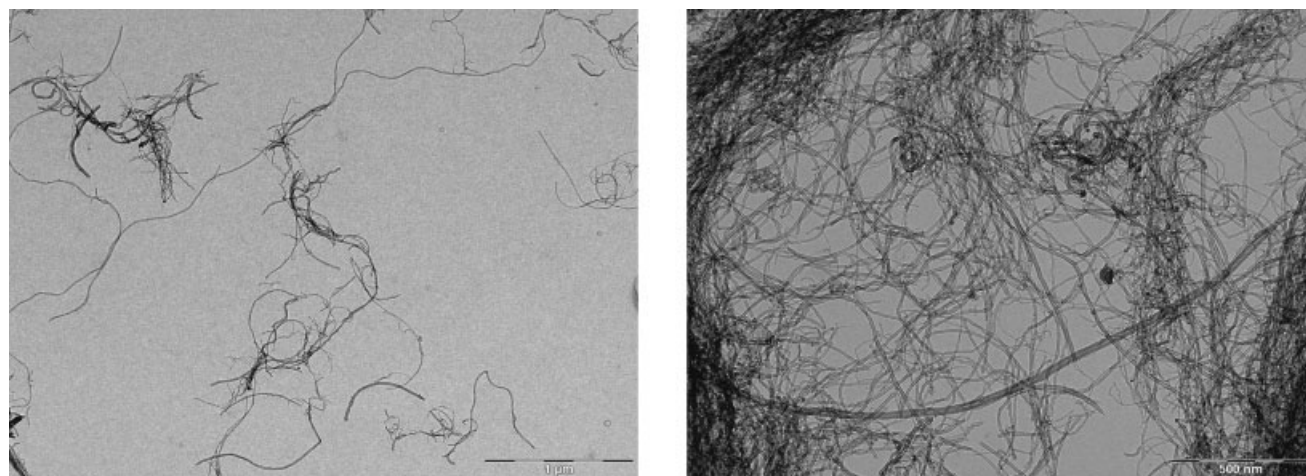**Figure 1** Stretching machine for electrical measurements under uniaxial extension.

Figure 2 TEM images of pure MWNTs.

tubes probably occuring during processing. These particle–particle interactions leading to aggregation or agglomeration as well as the orientation are of course, expected to affect the mechanical and electrical properties of the composite.

Additional information on how the nanotubes are actually being distributed within the polymer matrix can be obtained from atomic force microscopy. AFM has been shown to be particularly well suited for the characterization of filled elastomers and more generally of heterogeneous systems with components of different stiffness.[17] AFM images of SBR filled with 10 phr of MWNTs, shown in Figure 4, give some indication of a larger-scale dispersion than that given in Figure 3. The brighter domains easily identified and rather homogeneously distributed in the film, are ascribed to filler aggregates. It has to be recalled that topography and error signal reveal surface roughness while phase imaging, which provides variation of surface stiffness, is particularly useful in

elastomeric composites filled with carbon nanotubes on account of huge differences in moduli between the two components.

Mechanical properties

Tensile stress–strain curves for pure and MWNTs/ composites are represented in Figure 5. It can be seen that the modulus increases with the amount of carbon nanotubes. It should be noted that the particle agglomeration, as revealed by the TEM images, does not limit the increase in elastic modulus and also the increase in stress and strain at break except for the highest filler loading (10 phr) where a slight decrease in strain at rupture is observed.

Elastic moduli, determined from the slope of the curves representing the true stress against ($\alpha^2 - \alpha^{-1}$) (α being the extension ratio, which is the ratio of the lengths of the sample in the deformed and undeformed states) are listed in Table II. The stresses at
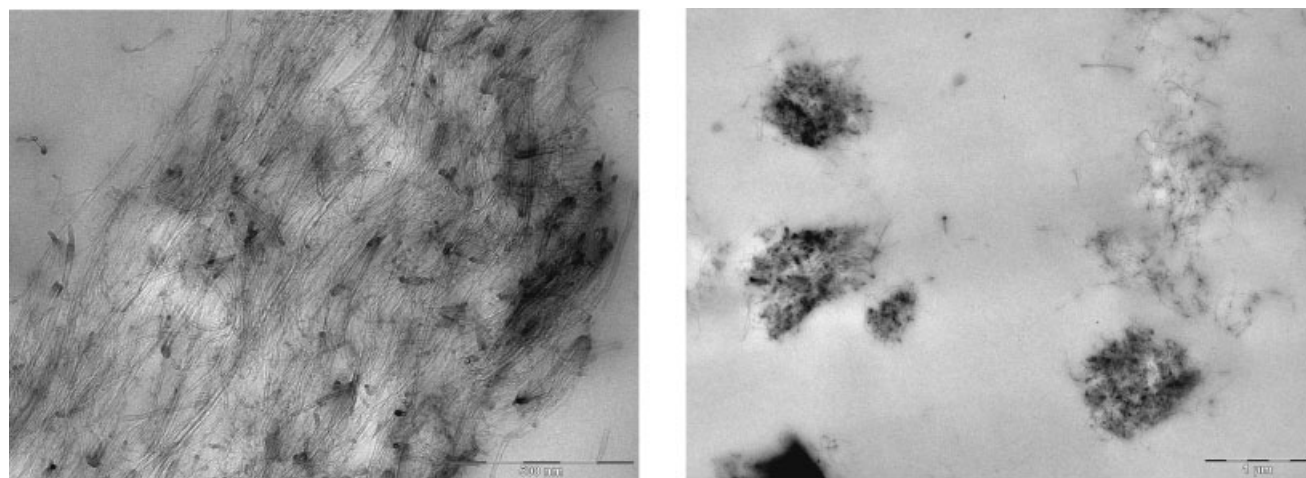

Figure 3 Transmission electron microscopy images of SBR filled with 4 phr of multiwall carbon nanotubes (MWNTs).
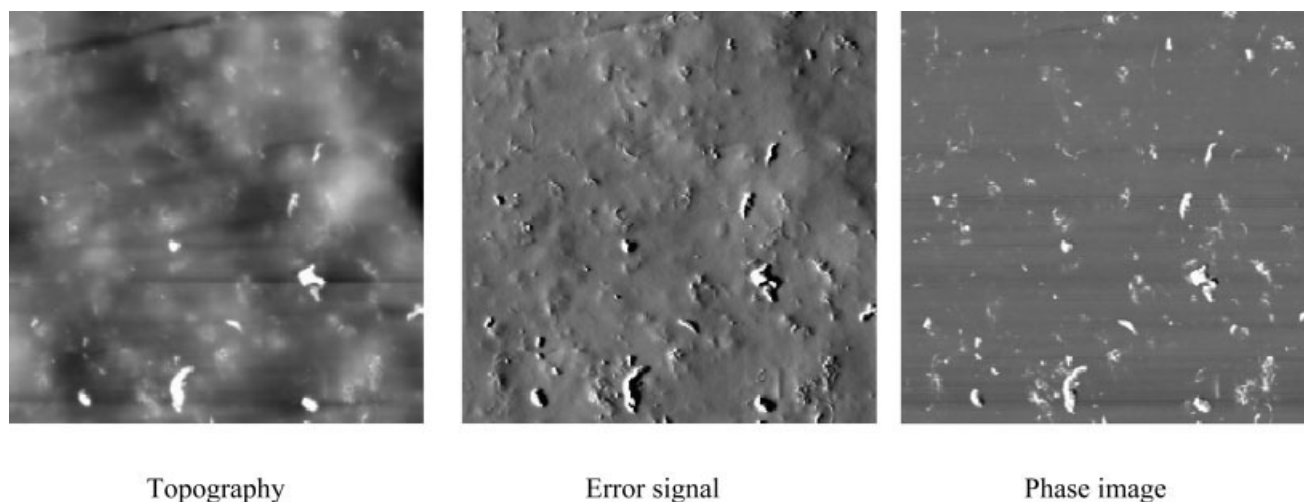
Topography   Error signal   Phase image

Figure 4 AFM images of SBR filled with 10 phr of multiwall carbon nanotubes (MWNTs). Full scale: 10 μm.

different strains as well as the stress and elongation at break are also reported.

Observation of the tensile data obtained for carbon black (CB) and MWNTs-filled samples [Fig. 6(a)] demonstrates that a small filler loading of MWNTs compared with CB is required to reach a same level of stress. This shows the enormous potential offered by the use of carbon nanotubes as reinforcing fillers if a successful dispersion throughout the polymer matrix can be achieved. But as seen in Figure 6(a), the ultimate strain of the MWNTs composites is significantly less than that obtained for those filled with CB, this can only be ascribed to the presence of agglomerates initiating cracks and limiting the tensile strength.

Besides the state of dispersion, an other fundamental issue that determines the properties of the composite is the interfacial interaction between the polymer and the nanotubes. A good adhesion between the two phases is required and might result in better load transfer from the matrix to the nanotube. An evaluation of the quality of the polymer-filler interface can be obtained from an estimation of the extent of stress-softening at large strains. This phenomenon which is characterized by a pronounced lowering in the stress when the sample is stretched a second time, takes place at the polymer-filler interface and is attributed, to a loss, by breakage or slippage of chains that have reached their limited extensibility, by strain amplification effects.[18] Quite similar hysteresis (area between the first and the second stretch) are obtained when SBR elastomer is filled with 10 phr of MWNTs or 50 phr of CB [Fig. 6(b)]. This would reflect equivalent matrix-filler interfaces. In nanotube-filled polymers, it is difficult to visualize or quantify the interaction zone since the agglomeration of the nanotubes results in a decrease of the effective interface area of the polymer-filler system. On the other hand,

the polymer adsorbed on the nanotube bundles or trapped inside a bundle might experience local stresses resulting in a debonding of the tube from the matrix or release of trapped rubber. Nevertheless, strain dependence of the Raman spectrum of SBR/MWNT composites did not give any evidence of a shift in the Raman band of the nanotubes upon uniaxial stretching,[19] which would be the signature of a weak interface between the two phases.

Electrical properties

The resistivity as a function of the carbon nanotubes content displays the typical dependency with the insulator-conductor transition corresponding to the region of the percolation threshold (Fig. 7). This tran-
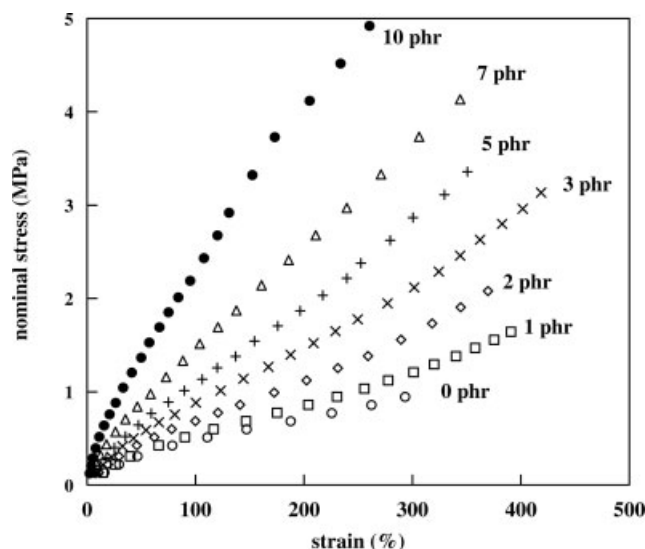

Figure 5 Stress–strain curves for pure SBR and MWNTs/SBR composites. The filler content is expressed in phr (phr, parts per hundred parts of rubber).

TABLE II
Mechanical Properties of SBR and SBR Composites

Filler loading (phr)	E (MPa)	Stress at 100% (MPa)	Stress at 200% (MPa)	Stress at 300% (MPa)	Stress at break (MPa)[a]	Strain at break (%)[a]
0	0.24	0.49	0.71	0.96	0.9–1.1	300–320
1	0.33	0.55	0.85	1.21	1.6–1.8	390–420
2	0.43	0.70	1.10	1.62	2.1–2.3	370–400
3	0.59	0.89	1.46	2.11	3.0–3.3	410–430
4	0.61	0.86	1.51	2.32	3.1–3.4	370–400
5	0.73	1.11	1.89	2.84	4.0–4.4	400–430
7	0.93	1.48	2.54	3.67	5.1–5.6	410–450
10	1.40	2.44	3.91	–	5.0–5.5	270–300

[a] Results of several test samples.

sition corresponds to the formation of a continuous interconnecting filler network. Above this critical filler loading, the resistivity is relatively low.

As seen in Figure 7, the critical concentration of conduction is between 2 and 4 phr, which is considerably less than that observed in carbon black-filled composites where values between 30 and 40 phr are reported.[20]
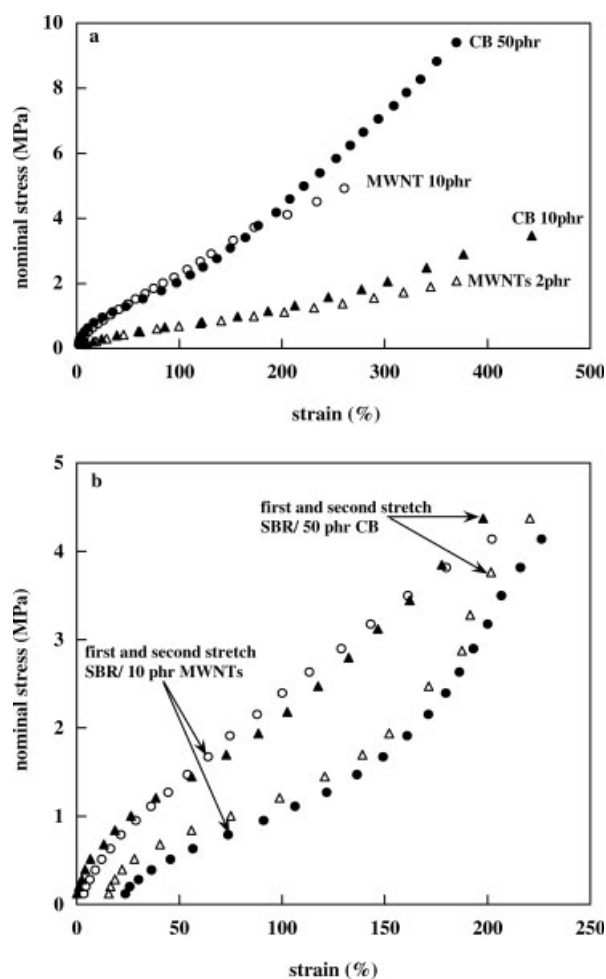
Owing to their high shape factor, carbon nanotubes are able to form a continuous network at a small filler loading. But aggregation of the tubes yields a conductive material at a higher volume fraction than that expected from individually dispersed MWNTs.

Changes in resistivity under uniaxial extension have been studied at deformations of up to 200% strain for the composite filled with 10 phr of MWNTs. It is observed that the resistivity of the sample increases gradually with the applied strain (Fig. 8). Our results differ from those presented by Yamaguchi et al.[16] for carbon black-filled elastomers where an increase in resistivity at low strains is observed, followed by a subsequent reduction at higher extensions. The authors explain the rise in the initial resistivity, by a breakdown of carbon black agglomerates into smaller aggregates, leading to a decrease in the total number of conduction paths.

As in the mechanical analysis, a second stretch was conducted after total unloading of the sample. As seen in Figure 8 and also reported in other stud-
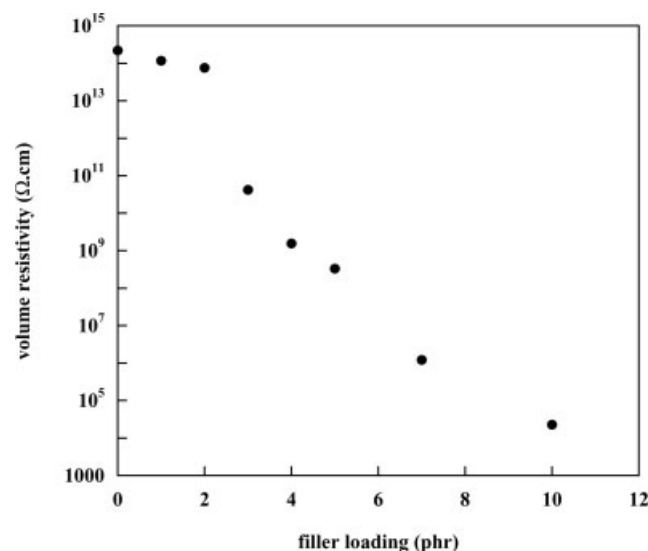

Figure 6 Comparison between MMNTs and CB filling effect on: tensile behavior (a) and Mullins hysteresis (b).

Figure 7 Volume resistivity against filler loading for SBR/MWNTs composites.
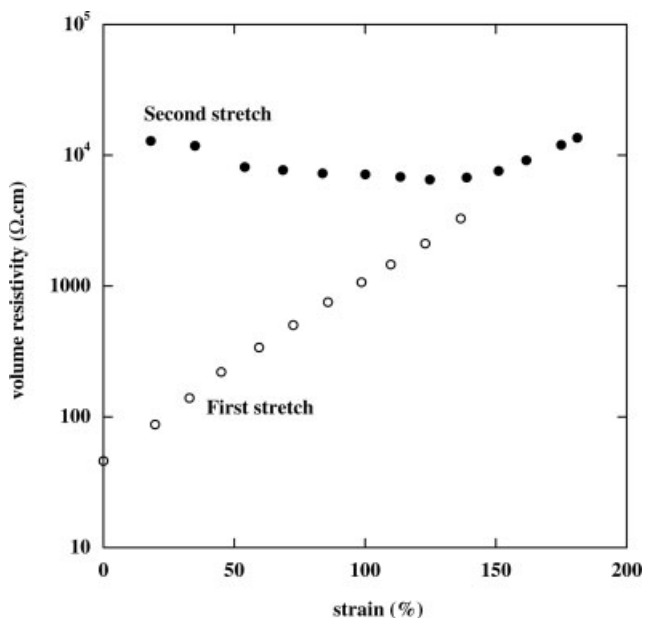
Figure 8 Strain dependence of the electrical resistivity for the SBR/10 phr MWNTs composite.

ies,[15,16] the resistivity of the fully relaxed composite, is significantly higher than that measured in the unstrained elastomer, showing that the filler network is not reformed after removal of the stress. For the second stretching, the resistivity slightly decreases and when the strain reaches the maximum value of the first stretching, the two curves coincide which

means that the sample is in the same state as it was at the first stretching. This hysteresis behavior, observed in electrical measurements, is seen to parallel the Mullins hysteresis in mechanical measurements but the former is associated with the filler network while the latter concerns the polymer-filler interface.

AFM investigations

Investigations by AFM under strain were undertaken to get further insight into the changes of the filler structure and correlate the electrical response with the AFM observations. AFM phase images obtained for two different extension ratio, α, are represented in Figure 9. It has first to be mentioned that the roughness increases with strain and the filler structures align in the direction of strain. These structures become more slender with the increase in extensional strain, resulting most probably in a loss of contacts between aggregates (or reduction in the number of conductive networks) and an increase in resistivity. On the other hand, an increase in extensional strain leads to a breakdown of nanotube bundles. The most striking results in this AFM investigation are those obtained after total release of the stress. Comparison between the original sample (Fig. 4) and the prestretched one (Fig. 10), both in the undeformed state, reveals a pronounced change in the morphology of the material. A second stretching per-
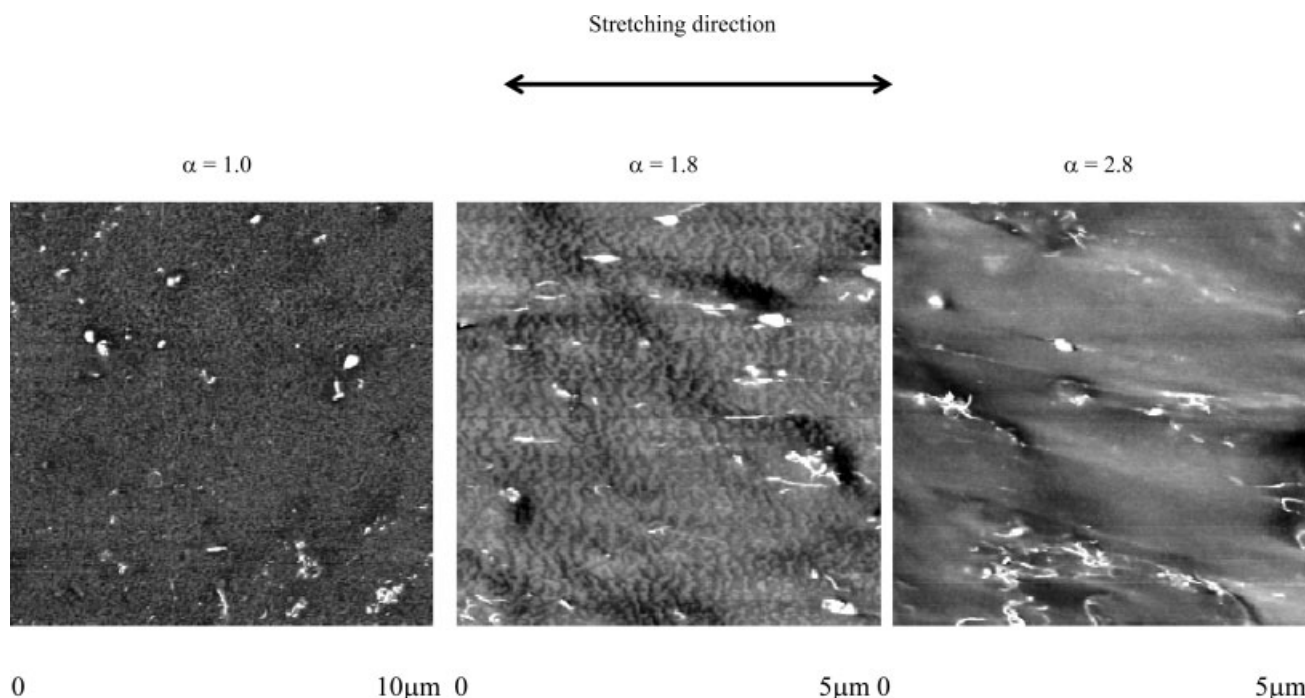

Figure 9 AFM images on unstretched and stretched films of SBR filled with 10 phr of multiwall carbon nanotubes (MWNTs): extension ratio α respectively, equal to 1, 1.8, and 2.8.
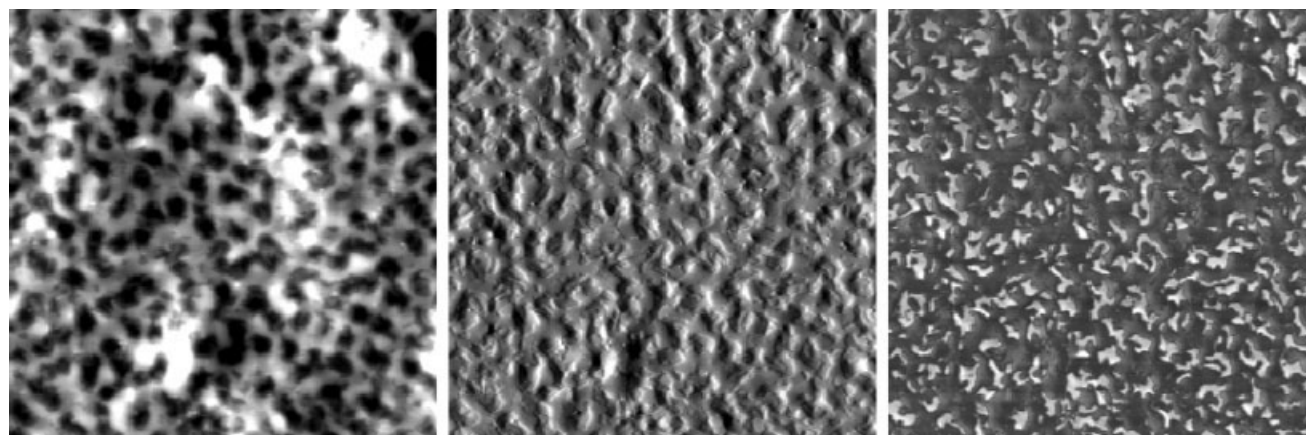
Figure 10 AFM images after total release of the stress. Full scale: 10 μm. Left, middle, and right images correspond respectively, to topography, error signal, and phase image.

formed on the sample does not display the same alignment as that observed for the first-stretched sample (Fig. 11). The second stretch reveals different arrangements in the filler structure: filler aggregates seem to be oriented perpendicularly to the stretching direction. In connection with the mechanical results, one has to keep in mind that a loss of elastic chains and consequently a decrease in modulus, is observed by prestretching the material. The strong alignment of the bundles perpendicular to the previous extension axis could be the result of a reequilibration of the stress field. Owing to filler structure reorientation and contraction during straining in the transverse direction, new conducting pathways are produced, leading to a weak decrease in resistivity. These observations, which bring new insights into the intriguing reinforcement imparted by carbon nanotubes, are still the subject of further investigations.

CONCLUSIONS

This study has demonstrated the intrinsic potential of carbon nanotubes as reinforcing filler in elastomeric materials. Despite a poor dispersion, small filler loadings substantially improves the mechanical and electrical behavior of the soft matrix. With the addition of 1 phr of multiwall carbon nanotubes in a styrene–butadiene copolymer, a 45% increase in modulus and a 70% increase in the tensile length are achieved. On the other hand, carbon nanotubes imparts conductivity to the insulator matrix. Between 2 and 4 phr, the conductivity increases by five orders of magnitude reflecting the formation of a percolating network. Changes in resistivity under uniaxial extension completed by AFM observations of stretched composites bring new insights into the properties of these composites by highlighting the contribution of orientational effects.
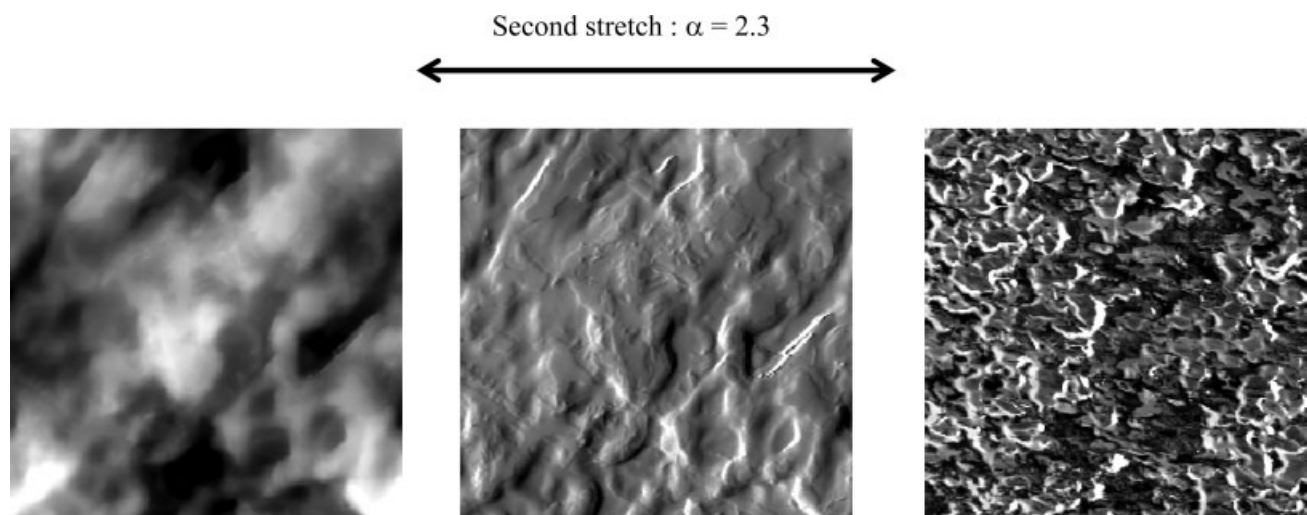
Second stretch : $\alpha = 2.3$

Figure 11 AFM images of SBR filled with 10 phr of multiwall carbon nanotubes (MWNTs): material stretched to $\alpha = 2.8$, released then restretched to $\alpha = 2.3$. Full scale: 5 μm. Left, middle, and right images correspond respectively, to topography, error signal, and phase image.

References

1. Dewimille, L.; Bresson, B.; Bokobza, L. Polymer 2005, 46, 4135.
2. Bokobza, L.; Chauvin, J.-P. Polymer 2005, 46, 4144.
3. Bokobza, L. Compos Interfaces 2006, 13, 345.
4. Bokobza, L.; Diop, A. L.; Fournier, V.; Minne, J.-B.; Bruneel, J.-L.; Macromol Symp 2005, 230, 87.
5. Schmidt, D. F.; Clément, F.; Giannelis, E. P. Adv Funct Mater 2006, 16, 417.
6. Ramanathan, T.; Liu, H.; Brinson, L. C. J Polym Sci Part B: Polym Phys 2005, 43, 2269.
7. Bokobza, L. Macromol Mater Eng 2004, 289, 607.
8. Bokobza, L. J Appl Polym Sci 2004, 93, 2095
9. Thostenson, E. T.; Ren, Z.; Chou, T.-W. Compos Sci Technol 2001, 61, 1899.
10. Sandler, J.; Shaffer, M. S. P.; Prasse, T.; Bauhofer, W.; Schulte, K.; Windle, A. H. Polymer 1999, 40, 5967.
11. Allaoui, A.; Bai, S.; Cheng, H. M.; Bai, J. B. Compos Sci Technol 2002, 1993, 62.
12. Bai, J. B.; Allaoui, A. Compos A 2003, 34, 689.
13. Du, F.; Fischer, J. E.; Winey, K. I. J Polym Sci Part B: Polym Phys 2003, 41, 3333.
14. Seoul, C.; Kim, Y.-T.; Baek, C.-K. J Polym Sci Part B: Polym Phys 2003, 41, 1572.
15. Das, N. C.; Chaki, T. K.; Khastgir, D. Polym Int 2002, 51, 156.
16. Yamaguchi, K.; Busfield, J. J.; Thomas, A. G. J Polym Sci Part B: Polym Phys 2003, 41, 2079.
17. Clément, F.; Lapra, A.; Bokobza, L.; Monnerie, L.; Ménez, P. Polymer 2001, 42, 6259.
18. Clément, F.; Bokobza, L.; Monnerie, L. Rubber Chem Technol 2001, 74, 847.
19. Bokobza, L.; Bruneel, J.-L. to appear..
20. Sau, K. P.; Chaki, T. K.; Khastgir, D. J Appl Polym Sci 1999, 71, 887.